Cu Interactions with α-Al_2O_3(0001): Effects of Surface Hydroxyl Groups vs. Dehydroxylation by Ar Ion Sputtering

C. Niu, K. Shepherd, D. Martini, J.A. Kelber*
Department of Chemistry, University of North Texas, Denton, TX 76203

D. R. Jennison and A. Bogicevic**
Surface and Interface Sciences Department, Sandia National Laboratories,
Albuquerque, NM 87185-1421

XPS studies and first principles calculations compare Cu adsorption on heavily hydroxylated sapphire (0001) with a dehydroxylated surface produced by Ar^+ sputtering followed by annealing in O_2. Annealing a cleaned sapphire sample with an O_2 partial pressure of ~5×10^{-6} Torr removes most contaminants, but leaves a surface with ~0.4ML carbon and ~0.4ML OH. Subsequent light (6 min.) Ar ion sputtering at 1 KeV reduces the carbon to undetectable levels but does not dehydroxylate the surface. Further sputtering at higher Ar ion excitation energies (>2 KeV) partially dehydroxylates the surface, while 5 KeV Ar ion sputtering creates oxygen vacancies in the surface region. Further annealing in O_2 repairs the oxygen vacancies in the top layers, but those beneath the surface remain. Deposition of Cu on the hydroxylated surface at 300 K results in a maximum Cu(I) coverage of ~0.35 ML, in agreement with theoretical predictions. Maximum Cu(I) coverage at 300 K decreases with decreasing surface hydroxylation. The results demonstrate that the degree of hydroxyl surface coverage critically affects the ability of Cu to "wet" sapphire(0001) at 300 K. In addition, first principles density functional calculations show that while an ad-OH species stabilizes Cu(I) at room temperature, any nearby in-surface OH does the opposite.

Keywords: Ab initio quantum chemical methods and calculations; Aluminum oxide; Chemisorption; copper; Sputter deposition; Wetting; X-ray photoelectron spectroscopy.

* Corresponding author. Fax: +1-940-369-8295. E-mail: kelber@unt.edu

** Present address, Ford Research Company, Dearborn, MI 48121-2053

I. Introduction

We report XPS studies which show that dehydroxylation of the α-Al_2O_3(0001) [sapphire(0001)] surface, by Ar^+ sputtering prior to Cu deposition, inhibits the formation of an initial Cu(I) conformal adlayer and promotes the formation of metallic Cu clusters. Furthermore, first principles calculations are used to study several varieties of hydroxylated surfaces and their affect on Cu adsorption at different coverages.

The interaction of metal adatoms with oxide substrates is of broad scientific and technological interest in areas such as heterogeneous catalysis, microelectronics, composite materials, and corrosion. A significant issue concerning the thermodynamics of the metal/oxide interaction is the strength of adatom binding compared with binding in two- or three-dimensional (2D or 3D) clusters on the oxide surface. For alumina surfaces, theoretical calculations indicate that all isolated metal adatoms transfer significant charge to the oxide[1, 2]. If the resulting oxidized adatom is sufficiently bound, this then results in layer-by-layer conformal growth of the metal (Frank-van der Merwe, FM, growth mode [3, 4]), at least for the first 1-3 layers (Stranski-Krastanov, SK, mode [3, 4]). A weaker interaction, on the other hand, would result in the formation of 3D metal clusters (Volmer-Weber, VW, mode [3, 4]). An additional issue concerns the kinetics of the deposition process. If the barriers for adatom diffusion are sufficiently large compared with the sample temperature, adatoms would be unable to diffuse to growing metal islands and a metastable FM structure could thus result.

Cu/Al_2O_3 interactions are of particular interest not only because of the technological relevance of this interface [5-7], but also because of inconsistencies in the reported results [8-18]. Combined AES, EELS and LEED studies showed the SK mode of Cu growth and Cu(I) formation (~2Å thick) on α-Al_2O_3(0001) [8-10], and XPS studies yielded similar conclusions [11]. In addition, a conformal overlayer of Cu on a thermally grown Al_2O_3 film on Al(111) was observed by AES and HREELS [12]. Another study of Cu interactions with a thermal Al_2O_3 film grown on polycrystalline Al indicated Cu-O ionic bond formation at less than 0.5 ML Cu coverage [13]. In contrast, some other studies of the Cu/α-Al_2O_3(0001) interface indicated that the interaction between Cu and the surface is weak, that Cu grows via the VW mode, and that metallic particles form from the very early stages of the Cu deposition [15-19]. The growth of Cu metallic clusters on ordered Al_2O_3 ultrathin films was also reported [14], and the observed change of X-ray generated Cu(LMM) Auger line shapes and Auger parameters with Cu coverage was explained as being the result of the final state screening effect [14, 16, 18, 19] instead of reflecting different oxidation states.

The above inconsistencies suggest that Cu nucleation and growth on Al_2O_3 is a complex balance between various factors which are not necessarily well-controlled, even in typical UHV environments. Early cluster calculations [20, 21] suggested that Cu/Al_2O_3 should be a weakly interacting system (resulting in non-wetting and formation of 3D metallic nuclei (VW growth) even at low

Cu coverages). However, recent thick slab calculations of metal/sapphire interactions [1] and ultrathin Al_2O_3 film structure [2] have demonstrated that very large relaxations occur in this system and these relaxations, not included in the cluster studies [20, 21], are critical for a correct energetic description. The above results have led to the present collaborative experimental/theoretical effort [22] to understand "real world" Cu/Al_2O_3 interfaces.

In a previous study [22], we presented results from both density functional large slab calculations and experimental XPS which demonstrate that Cu will wet a hydroxylated α-Al_2O_3 (0001) (θ_{OH}=0.47ML) surface at 300K. An initial Cu(I) adlayer was observed with a maximum coverage of ~0.35ML (on a Cu/O atom basis), in excellent agreement with theory. At higher Cu coverages, a second, metallic Cu overlayer was observed to form over the initial Cu(I) adlayer. The calculations also indicated that thermodynamically and kinetically Cu should not wet a dehydroxylated α-Al_2O_3 (0001) surface at 300K, and suggested that the results should be sufficiently general as to apply to other metal/alumina systems.

In this report, XPS data are presented which show that maximum Cu (I) coverage at 300 K decreases with decreasing OH surface coverage. Dehydroxylation is accomplished by Ar^+ ion bombardment, followed by annealing in a partial pressure of O_2. Cu (I) formation on dehydroxylated sapphire(0001) is inhibited at 300K, with Cu(0) formation and 3D (VW) growth preferred. These data demonstrate that the degree of surface hydroxylation is indeed critical to the wetting behavior of Cu on the sapphire(0001) surface. The data also substantiate the predictions [22] of large slab calculations of Cu behavior on dehydroxylated sapphire(0001).

The atomic-scale structure of the hydroxylated sapphire surface is in fact unknown. However, its stability to over 1000K [22], which is not observed when a clean surface is hydroxylated in vacuum using a water plasma[23], suggests a crystalline form of aluminum hydroxide or oxy-hydroxide, where the greater stability can be explained as arising from a Madelung potential. In general, one can conceive of two types of surface OH groups: ad-OH, which exist entirely above the surface, and in-surface OH, which are contained within the surface layer. In the case of water dissociation on sapphire(0001), one would expect one of each type to be made[24], the in-surface species arising from the reaction of H^+ with an O^{2-} ion. Here, using first principles slab calculations, we also investigate how each type of OH species affects the binding of Cu adatoms and a layer of Cu metal.

Section II contains a description of experimental and theoretical methods. Results are presented in section III, and a discussion is contained in section IV. Summary and conclusions are presented in section V.

II. Experimental and theoretical methods

Experiments were carried out in a combined UHV analysis/magnetron sputter deposition system which has been described previously [22]. To tolerate high gas loading, the analysis and sputter deposition chambers were independently

evacuated by turbomolecular pumps. Pressures in both chambers (in the absence of plasma) were monitored by nude ion gauges placed out of the line of sight from the sample. Base pressures were 7×10^{-10} Torr in the analysis chamber and 2×10^{-8} Torr in the deposition chamber. Typical working pressures were $1\text{-}5\times10^{-9}$ Torr in the analysis chamber and 4×10^{-8} -1×10^{-7} Torr in the deposition chamber. Pressures during plasma induced sputter deposition were monitored with a baratron gauge. A metal gate valve separated the two chambers when the sample was drawn out from analysis chamber to deposition chamber. Chamber isolation during sample analysis was achieved with differentially pumped Teflon seals against the polished double-walled manipulator rod.

The samples were $10 \times 10 \times 0.5$ mm square slabs of α-Al_2O_3 (Princeton Scientific) with one (0001) face polished optically flat. The samples were cleaned by sonication in acetone, methanol and deionized water consecutively prior to being mounted on a tantalum sample holder. The two tantalum leads of the sample holder were in contact with a liquid nitrogen reservoir. A combination of liquid nitrogen cooling and resistive heating of the sample holder permitted a variation of sample temperature between 130 K and 1200 K. Sample temperatures were monitored by a K-type thermocouple, spot-welded at an edge of the sample holder and bent so that the junction was in contact with the sample surface.

XP spectra were acquired using a VG100AX hemispherical sector analyzer operated at a constant pass energy of 50 eV. Calibration of the analyzer energy scale was carried out using sputter cleaned Cu and Au samples according to established techniques[25]. Mg Kα X-ray radiation was obtained from a commercial, unmonochromatized source (Physical Electronics, PHI model 1427) operated at 15 kV and 300 W. Software for data acquisition and analysis have been described previously [26]. XPS spectra were acquired with the sample aligned normal to the analyzer lens axis (normal incidence) and at 60° with respect to the normal incidence (grazing incidence). The sapphire samples showed significant differential charging [27-31], which is common in XPS studies of insulating materials. The details have been discussed elsewhere [22]. Briefly, the degree of charging for a given peak is a function of the inelastic mean free path (IMFP) and the take-off angle. Greater charging is observed for longer IMFP and normal incidence. Correction for such differential charging is more problematic than that for uniform charging, and this makes it difficult to obtain the exact binding energies. In this paper, all the binding energies are reported without charging corrections. Characterization of Cu oxidation states is based on X-ray excited Auger spectral line shape instead of the absolute binding energies. The Cu Auger parameters (AP) were calculated according to the following:

$$1) \quad AP = KE(Cu_{LMM}) + BE(Cu_{2p})$$

$$2) \quad KE(Cu_{LMM}) = h\nu - BE(Cu_{LMM})$$

where KE and BE are kinetic energy and binding energy respectively. Although Auger parameters are insensitive to uniform charging, our results show that

they are affected by differential charging. The APs reported in this paper are not comparable with literature values. Again, our conclusions depend more on the Cu_{LMM} line shapes than the absolute AP values.

A sputter ion gun (Physical Electronics, PHI model 04-191) in the analysis chamber was operated by direct argon gas feed into the ionization chamber with a variable excitation voltage of 1 – 5 KeV. The samples were first annealed to 1100K for 1 hour in 5×10^{-6} Torr O_2, then exposed to brief Ar^+ bombardment (1 KeV) in order to remove adventitious carbon. Prior to Cu deposition, the samples were again annealed to 1100 K in 5×10^{-6} Torr O_2. Such a procedure is reported [23] to result in a sharp (1×1) hexagonal LEED pattern. Our previous XPS results [22] show that after the above treatment, the Al_2O_3(0001) surface is carbon free but still substantially hydroxylated. Cu deposition was carried out using a commercial water-cooled magnetron source (MiniMak) and an Argon plasma with a partial pressure of 0.015 Torr. The deposition rate could be controlled by adjusting the plasma power, and was shown to be highly reproducible. All Cu depositions reported in this paper were done at room temperature (~300 K).

The theoretical work used density functional theory [32, 33] in the local density approximation (LDA) [34, 35], as implemented in the Vienna Ab-Initio Simulations Package (VASP) [36-38]. Ultrasoft Vanderbilt pseudopotentials [39, 40] accurately replaced the core electrons at a plane wave cutoff of only 270 eV. Geometric relaxation was made using a damped molecular dynamics algorithm, until all forces were less than 0.05 eV/Å. The sapphire slab had six layers of the alumina unit cell, thus having six oxygen and twelve aluminum layers. The adsorbates were placed on one side, with the bottom three unit cell layers frozen in position at the bulk LDA geometry, which is within 0.2% of experiment. Because of long-range electrostatic interactions, the vacuum gap between the vertically repeating slabs always exceeded 18 Å.

III. Results

A. Vicinal and sputtered sapphire (0001) surfaces

Figure 1 shows a survey scan (normal incidence) for an initial sapphire sample, and a scan after annealing to 1100 K for 1 hour in 5×10^{-6} Torr O_2. The samples were initially covered by multi-layers of carbon, which indicates that either the ultra-sonic clean with acetone, methanol and deionized water was not enough to remove all the carbon on the sample completely, or carbon containing species saturated the surface immediately after cleaning. The annealing in oxygen significantly reduced the C(1s) signal. However, the remaining 0.4 ML C (based on the C to O atomic ratio, see Figure 1.b) was so stable that another hour of annealing in O_2 could not further reduce it. Ar^+ sputtering at 1KeV excitation energy and 25mA emission current for 6 minutes reduced the remaining carbon to undetectable levels.

The O(1s)/Al(2p) ratio after various annealing and Ar^+ sputtering treatments are summarized in Table I. In all cases grazing incidence XPS gave a

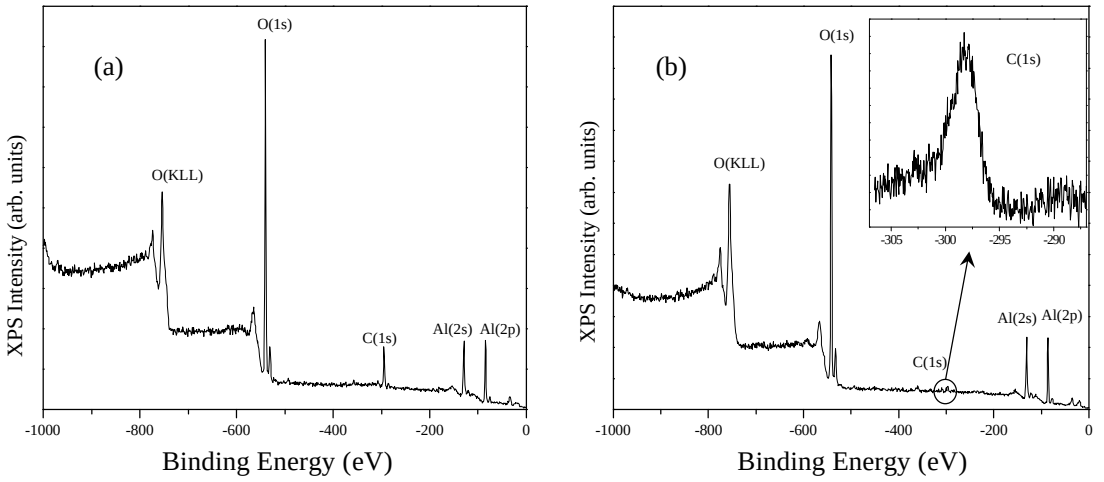

Fig. 1. XPS survey scans of (a) an initial sapphire(0001) sample, and (b) the sample after 1 hour annealing in 5 x 10^{-6} Torr O_2. Annealing removed most contaminants but left ~0.4ML strongly bound carbon on the surface.

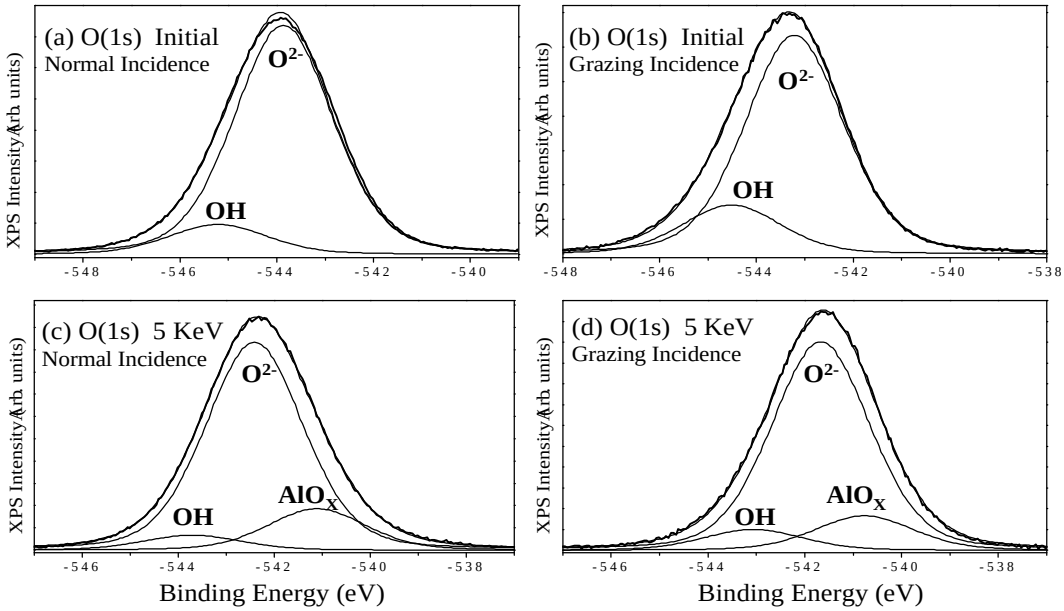

Fig. 2. O(1s) spectra (without charging correction) of initial and 5 KeV Ar+ sputtered sapphire(0001) surface: (a) Initial, normal incidence; (b) Initial, grazing incidence; (c) 5 KeV sputtered, normal incidence; and (d) grazing incidence. The samples were all annealed in 5×10^{-6} Torr O_2 for 1 hour at 1100K before XPS analysis.

higher O(1s)/Al(2p) ratio. Since the average sampling depth for 60 degree grazing incidence is only a half of that for normal incidence, we conclude that there was oxygen enrichment on the surface. Annealing at 1100 K for one hour in UHV or in 5 × 10^{-6} Torr O_2 resulted in the same O(1s) and Al(2p) spectra and O(1s)/Al(2p) ratio. The O(1s) and Al(2p) spectra are shown in Figure 2 and Figure 3, respectively. The O(1s) spectra are well fit by two components

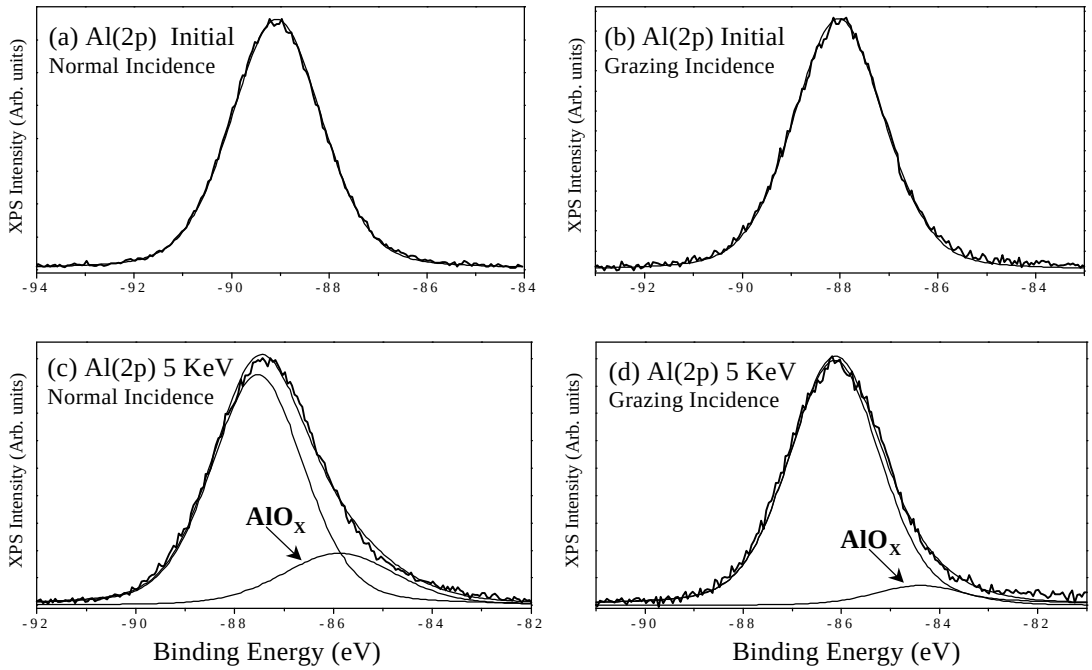

Fig. 3. Al(2p) spectra (without charging correction) of sapphire(0001): (a) Initial, normal incidence; (b)Initial, grazing incidence; (c) 5 KeV sputtered, normal incidence and (d) grazing incidence. The initial spectra are well fit by a single peak with FWHM of 2.2 eV. After 5 KeV Ar+ sputtering a metallic Al peak appeared at 1.7eV lower binding energy than the main peak. The percentage of Al(0) peak area (21.3% for normal incidence and 7.5% for grazing incidence) showed that the Al(0) was located beneath the surface layer which itself was fully oxidized.

each with FWHM of 2.4 eV, a main peak and a minor peak at 1.3 eV higher binding energy. In agreement with a previous report [11], the relative intensity of the high-energy peak is increased at grazing incidence, which indicates that this component corresponds to a surface species. Based on the known fact that the sapphire surfaces are difficult to make hydrogen free [24, 41, 42], we attribute this peak to surface hydroxylation. The 1.3 eV difference between the OH and main O(1s) features is in good agreement with previous reports [11]. These OH groups were sufficiently stable that they could not be removed either by another hour of annealing at 1100 K or by 6 minutes Ar^+ sputtering at 1 KeV. The hydroxyl coverage was estimated to be ~0.47 ML using a method discussed previously [22]. Ar^+ sputtering at 2 KeV for 10 minutes, on the other hand, was able to reduce the OH component to about 2/3 of the original value. The Al(2p) spectra did not change after 1 KeV or 2 KeV sputtering, and could be well fit by a single component. Both the O(1s) and Al(2p) spectra were stable upon subsequent annealing to 1100 K in O_2.

As shown in Table I, significant changes of the O(1s) and Al(2p) spectra occurred after 10 minutes Ar^+ sputtering at 5 KeV followed by annealing in O_2. The O(1s)/Al(2p) intensity ratio decreased by 10% for grazing incidence (from 6.4 to 5.8). Subsequent annealing in O_2 increased this ratio by 2%, indicating a reaction of O_2 with the sputtered surface. Sputtering caused both O(1s) and Al(2p) spectra became wider (Figs. 2 and 3). The OH component decreased to about a half of the initial

Table I. O(1s)/Al(2p) intensity ratio (± 0.1) after various treatment of the sapphire(0001 surface. Ar^+ sputtering time was 6 minutes for 1 KeV, and 10 minutes for 2 and 5 KeV Annealing was done at 1100K for 1h with $pO_2 = 5\times10^{-6}$ Torr. Subsequent annealing in O after 1, 2 KeV sputtering did not change the O(1s)/Al(2p) intensity ratio.

Sample treatment	Initial sample	Annealed in O_2	Sputtered at 1 KeV	Sputtered at 2 KeV	Sputtered at 5 KeV	Sputtered at 5 KeV, then annealed in O_2
Normal incidence	5.9	5.8	5.8	5.8	5.6	5.7
Grazing incidence	6.2	6.4	6.4	6.2	5.8	5.9

value. Another component appeared at a binding energy 1.1 eV lower than the main oxygen peak. The emergence of this component coincided with the partial reduction of Al^{3+}, as shown in Figure 3(c) and 3(d). The metallic Al(2p) feature is more prominent in the normal incidence spectrum, its contribution to the total Al(2p) area being about 21%, in contrast to 8% in the grazing incidence case. This difference is an indication that the metallic Al on the surface was oxidized during O_2 annealing, while that beneath the surface remained. The low binding energy O(1s) peak also showed enrichment beneath the surface, and we assign it to the oxygen bound to the partially reduced aluminum. The charging decreased by ~1.7 eV for both O(1s) and Al(2p) peaks after 5 KeV Ar^+ sputtering, as shown in figs. 2 and 3, which may be an effect of partial aluminum reduction.

The above results show that Ar^+ sputtering at energies higher than 2 KeV decreases the surface hydroxyl concentration. The changes in the O(1s) and Al(2p) spectra indicate that oxygen vacancies were created by Ar^+ sputtering. Subsequent annealing in O_2 refills the vacancies in the top layer(s), but a significant amount of partially reduced Al remained beneath the surface. Any changes to surface topography, of course, cannot be determined from the data.

B Cu nucleation studies

Copper deposition was performed on sapphire(0001) surfaces after different treatments: (a) annealing in O_2 only (θ_{OH} = ~0.47 ML); (b) 1 KeV Ar^+ sputtering , then annealing in O_2 (θ_{OH} = ~0.47 ML); (c) 2 KeV Ar^+ sputtering, then annealing in O_2 (θ_{OH} = ~0.31 ML); (d) 5 KeV Ar^+ sputtering, then annealing in O_2 (θ_{OH} = ~0.23 ML). The deposition rate was controlled to be constant at 0.03 ML per minute. After every 2 minutes of deposition, the sample was transferred to the analysis chamber and XPS was used to monitor the growth of Cu. The evolution of the X-ray excited Cu(LMM) Auger electron spectrum with deposition time is shown in Figure 4. There are two distinguishable features with AP (Auger parameter) values of 1843.9 and 1847.3 eV. Literature [43] AP values for Cu(I) and Cu(II) are ~1849.1 and 1851.3 eV respectively. The difference between observed Auger parameters and literature values is attributed to differential charging, as previously reported [22]. No shake-up satellite peaks that are characteristic for Cu(II) [11, 43, 44] were observed in the Cu(2p) spectra (Figure 5).

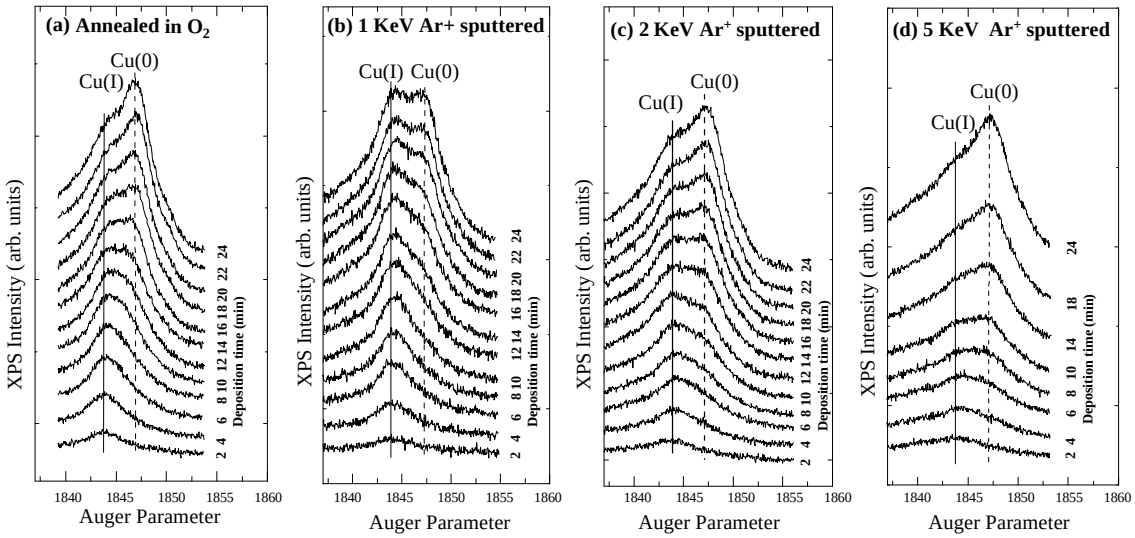

Fig. 4. X-Ray excited Cu(LMM) evolution during Cu deposition on sapphire(0001): (a) annealed in O_2 only, (b) 1 KeV lightly sputtered, (c) 2 KeV sputtered, and (d) 5 KeV heavily sputtered. All were annealed in O_2 before Cu deposition. Dehydroxylation of the surface resulted in the decrease of the Cu(I) component.

After annealing an as-received sample, the remaining 0.4 ML of C on the surface apparently occupied some active sites and prevented Cu(I) formation [Fig. 4a]. Brief 1 KeV Ar^+ sputtering resulted in a carbon free surface. The Cu(2p)/O(1s) intensity ratio as a function of Cu sputter deposition time are displayed in Fig. 6 for 1 KeV and 5 KeV sputtered surfaces. Results obtained for the 2 KeV sputtered surface were intermediate between the two cases shown, but are omitted in Fig. 6 for clarity. In all cases, the uptake curve shows a sharp break, which indicates the end of a conformal initial growth stage. A comparison of Figs. 5 and 6 indicates that Cu(I) is initially formed, with subsequent formation of Cu(0). The maximum coverages of Cu(I) are 0.35, 0.24, and 0.12 ML for 1, 2, and 5 KeV

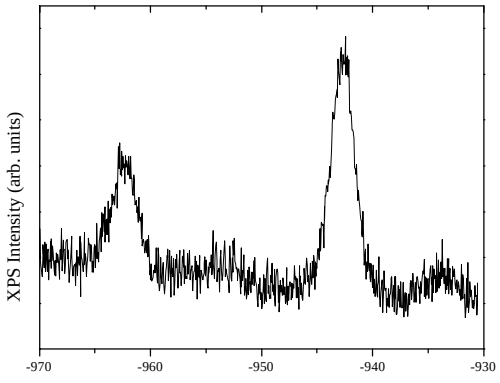

Fig. 5. Cu(2p) spectrum at Cu coverage of 0.06ML (based on Cu/O atomic ratio). No shake-up satellite peak that is characteristic of Cu(II) was observed.

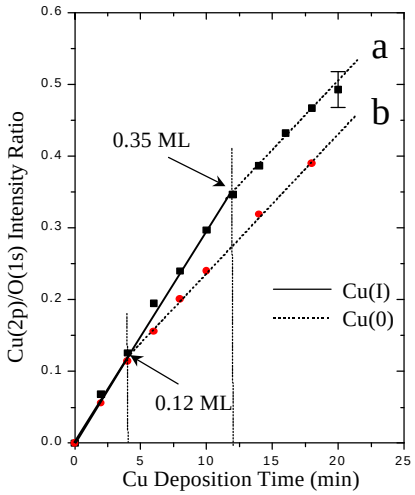

Fig. 6. Uptake curves of Cu on (a) 1 and (b) 5 KeV Ar^+ sputtered sapphire(0001). The breaks coincided with the Cu(LMM) lineshape changes. The growth of Cu(I) stopped much earlier in the case of 5 KeV sputtered (and dehydroxylated)surface.

Table II. Cu coverage (ML) for maximum conformal Cu(I) growth and for equal Cu(I) ai Cu(0) intensity in Cu(LMM) spectra.

Sample treatment	Annealing in O_2 only	1KeV Ar^+ sputtering + annealing in O_2	2KeV Ar^+ sputtering + annealing in O_2	5KeV Ar^+ sputtering + annealing in O_2
Conformal Cu(I)	0.24	0.35	0.24	0.12
$I_{Cu(I)} = I_{Cu(0)}$	0.48	0.72	0.48	0.24

Table III. Cu adatom binding energies, in eV on a per atom basis, for different sapphire (0001) surfaces. OH(a) is ad-OH, OH(s) is in-surface OH; if present, all are at 1/3 ML.

Species	Clean	Clean+OH(a)+OH(s)	Clean+OH(a)
Cu 1/3ML	1.8	1.8	5.2
Cu 1ML	0.5	0.3	1.2

Ar^+ sputtered surfaces respectively (Table II).

C. Theoretical studies

In Table III, we report the computed LDA binding energies (on a per atom basis) for adsorbed Cu (oxidized adatoms at 1/3 ML coverage and metallic Cu at 1ML coverage) on different surfaces. The following cases were considered: 1) a clean sapphire surface, 2) clean plus 1/3 ML of ad-OH and 1/3 ML of in-surface-OH (as would be produced by the

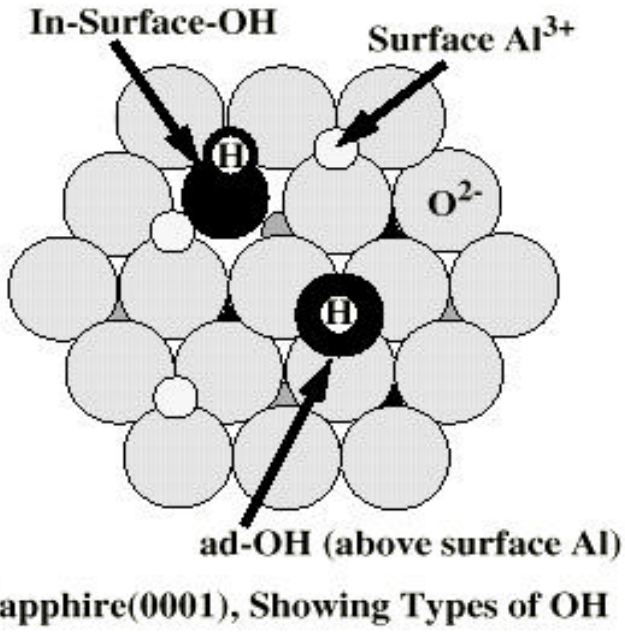

Figure 7. The α-Al_2O_3(0001) surface showing an example of the in-surface and the ad-OH species. The ad-OH prefers to sit directly above a surface Al ion, while the in-surface species tilts somewhat to further separate the positive hydrogen region from the neighboring Al sites.

dissociation of 1/3 ML of water [24], and 3) clean plus 1/3 ML of ad-OH. (See Fig. 7 for a visualization of these species.) It is seen that the in-surface species (cf. surfaces #2 and #3) weakens the adatom binding to the point where it almost exactly counteracts the strengthening affect of ad-OH (cf. #2 and #1). Indeed, the latter species sufficiently strengthens adatom binding (cf. #3 and #1) to: a) reverse the Born-Haber cycle prediction of not wetting the clean surface [22], and b) presumably pin the adatoms at room temperature so diffusion across the surface does not occur. Indeed, it would cost ~ 3 eV in energy for the adatom to separate from the ad-OH.

Finally, noting the strong increase in adatom binding that would occur on surface #2 if the in-surface-OH would give up its hydrogen, we computed the energetics of the reaction $2Cu(a) + 2OH(a) + 2OH(s) \rightarrow 2Cu(a) + 2OH(a) + H_2(g) + 2O(s)$, where a, g, and s stand for adsorbed, gas, and in-surface species, respectively. We find that it is exothermic by 0.8 eV (LDA) for the presence of two Cu adatoms to cause the dissociation of neighboring in-surface OH and the evolution of hydrogen gas. However, because LDA overbinds the hydrogen molecule to an unusual extent, it is likely that the actual energy released would be less.

IV. Discussion

The data show that the extent of Cu(I) formation on α-Al_2O_3(0001) at 300K decreases with decreasing hydroxyl coverage. On a carbon free, substantially hydroxylated surface (θ_{OH} = ~0.47 ML), deposited Cu grows conformally as Cu(I) to a maximum coverage of ~0.35ML, in accord with theoretical predictions [22] of a maximum coverage of 0.33ML, limited by Cu(I) –Cu(I) repulsion (Fig. 4b, Fig. 6). Reducing the initial OH coverage reduces the corresponding maximum Cu(I) coverage at 300K (Table II, Fig.6). This clearly demonstrates that the formation of Cu(I) at the sapphire(0001) surface at 300K is due specifically to the interaction of Cu adatoms with hydroxyl groups. These data therefore provide an explanation for the inconsistencies in the literature concerning Cu(I) observation [5-7] and also the reports of Cu wetting vs. non-wetting of alumina surfaces [8-18]. A related interaction has been reported for Rh on hydroxylated alumina thin films [7], where it has been suggested that ad-OH groups serve to nucleate metal islands. While this claim has been supported by theoretical calculations of metal dimer stability [45], the OH density in Ref. [7]was apparently much less than that reported here.

The nature of hydroxyl groups on sapphire(0001) surfaces, and their thermal stability, is itself a matter of some controversy. Several publications [23, 46] report that all OH groups formed by the exposure of sapphire(0001) surfaces to water vapor in vacuum are removed by heating to ~600K, in agreement with studies on alumina powdered samples and thin films [47]. In contrast, ion scattering studies [41] indicate that substantial surface hydroxylation can persist even after heating above 1400K. The latter results are in accord with our previous results [22] and those reported here as, in our experiments, surface hydroxylation was not removed by annealing in UHV to

1100K. At least part of the reason for this discrepancy may be the possibility of several different types of OH containing structures on a sapphire(0001) substrate. Supporting evidence for this explanation derives from the different OH XPS binding energies observed when hydroxylation occurs by different means: When produced by exposure to water vapor under UHV or high vacuum conditions, a binding energy ~2.0eV higher than the main O(1s) peak is found[48]. Exposure at near-atmospheric pressure results in a binding energy only 1.7eV from the main O(1s) feature, consistent with the formation of an aluminum hydroxide phase [48]. The OH feature observed in our studies displays a 1.3eV shift from the main O(1s) peak, in agreement with a 1.4eV shift reported in a previous XPS study [11]. In our case, surface hydroxylation is certainly due to exposure of the sapphire surface to the atmosphere prior to introduction into the vacuum chamber, rather than to the chamber ambient. In fact, exposure of a dehydroxylated surface to the ambient of either the UHV or sputter deposition chambers resulted in no significant increase in surface hydroxyl coverage. The correspondence between the feature reported here (1.3eV removed from the main peak), however, and that of the 1.7eV-shifted feature previously reported [48] as resulting from high pressure water vapor exposures, cannot be determined from the existing data.

The theoretical results indicate that the increased stability of Cu(I) in the presence of ad-OH is due to a deepening of the electrostatic well in which the oxidized, positively charged, Cu sits. This is caused by the addition of a negatively charged lateral neighbor. In contrast, the presence of a neighboring in-surface-OH reduces the binding compared with the perfect surface, because a neighboring charge is reduced from ~ –2 (an oxygen ion) to ~ –1 (the OH). The calculations show, if a surface were saturated with even amounts of both types of OH, the net effect on the heat of adsorption of Cu adatoms would be close to zero, in agreement with recent microcalorimetry experiments [49]. However, our calculations also indicate that if Cu were to be deposited on such a surface, the in-surface species could be depleted, because it is energetically favorable to dissociate the in-surface species, releasing hydrogen gas, and thus strongly increasing the binding of nearby Cu adatoms.

The data do not reveal any loss in OH due to the Cu/OH interaction. XPS spectra taken after Cu deposition and after annealing (to induce Cu dewetting), show no observable change of OH intensity, whereas a decrease in OH surface coverage is observable after Ar^+ bombardment. The data therefore suggest that Cu(I) formation is not accompanied by OH decomposition. While the lack of resolution of the OH feature in the O(1s) spectra (e.g, Fig. 2) limits the definitiveness of such a conclusion, if ad-OH and in-surface-OH were present in comparable numbers, we could not explain the increase in ad-Cu binding necessary to permit Cu(I) to be observed at room temperature and be stable to > 1000K. We therefore suggest that the hydroxylated surface studied here is an aluminum oxy-hydroxide film on sapphire, consisting largely of a close packed plane of O^{2-} (with a normal component of neighboring Al ions) but a substantial coverage of ad-OH above that

plane. Further structural details remain unknown.

V. Conclusion

Experimental studies have examined the effects of surface dehydroxylation on the interactions at Cu/α-Al_2O_3(0001) interface. The results indicate:

(1) Ar^+ sputtering at 2 KeV or higher resulted in dehydroxylation of the surface;
(2) Ar^+ sputtering at 5 KeV creates oxygen vacancies in the surface region. Only vacancies in the top layer(s) can recover by subsequent annealing in O_2, while those beneath the surface remain.
(3) Dehydroxylation of sapphire(0001) results in weaker overall Cu/Al_2O_3 interaction. Conformal growth of Cu(I) stops earlier and formation of Cu(0) clusters dominates thereafter.
(4) The hydroxylated surface produced by atmospheric exposure contains ad-OH groups which stabilize Cu adatoms, while in-surface OH groups, which destabilize Cu adatoms, are absent or are a minority species.

Acknowledgements:

VASP was developed at the Institut für Theoretische Physik of the Technische Universität Wien. Work at UNT was supported in part by the U.S. Department of Energy, Office of Basic Energy Sciences, under Grant No. DE-FG03-93ER45497, and in part by the Robert Welch Foundation, under Grant No. B-1356, which are gratefully acknowledged. Sandia is a multi-program laboratory operated by Sandia Corporation, a Lockheed-Martin Company, for the U. S. Department of Energy under Contract DE-AC04-94AL85000. This work was partially supported by a Laboratory Directed Research and Development Project.

References

[1] C. Verdozzi, D. R. Jennison, P. A. Schultz, M. P. Sears, Phys. Rev. Lett. 82 (1999) 799.
[2] A. Bogicevic, D. R. Jennison, Phys. Rev. Lett. 82 (1999) 4050.
[3] C. Argile, G. E. Rhead, Surf. Sci. Rep. 10 (1989) 277.
[4] L. C. Feldman, J. W. Mayer, Fundamentals of Surface and Thin Film Analysis, P T R Prentice-Hall, Inc. 1986.
[5] National Technology Roadmap for Semiconductors, Semiconductor Industry Association 1997.
[6] M.-C. Wu, D. W. Goodman, J. Phys. Chem. 98 (1994) 9874.
[7] G. Ertl, H.-J. Freund, Physics Today 52 (1999) 32.
[8] Q. Guo, P. J. Moller, Surf. Sci. 244 (1991) 228.
[9] Q. Guo, P. J. Moller, L. Gui, Acta Physica Polonica A 81 (1992) 647.
[10] P. J. Moller, Q. Guo, Thin Solid Films 201 (1991) 267.
[11] S. Varma, G. Chottiner, M. Arbab, J. Vac. Sci. Technol. A 10 (1992) 2857.
[12] J. G. Chen, M. L. Colaianni, W. H. Weinberg, J. J.T. Yates, Surf. Sci. 279 (1992) 223.
[13] F. S. Ohuchi, R. H. French, R. V. Kasowski, J. Appl. Phys. 62 (1987) 2286.
[14] Y. Wu, E. Garfunkel, T. E. Madey, J. Vac. Sci Technol. A 14 (1996) 1662.

[15] S. Gota, M. Gautier, L. Douillard, N. Thromat, J. P. Duraud, P. L. Fevre, Surf. Sci. 323 (1995) 163.
[16] M. Gautier, L. P. Van, J. P. Duraud, Europhys. Lett. 18 (1992) 175.
[17] M. Gautier, J. P. Duraud, L. P. Van, Surf. Sci. Lett. 249 (1991) L327.
[18] V. Vijayakrishnan, C. N. R. Rao, Surf. Sci. Lett. 255 (1991) L516.
[19] A. F. Carley, M. K. Rajumon, M. W. Roberts, J. Solid State Chem. 106 (1993) 156.
[20] V. D. Castro, G. Polzonetti, R. Zanoni, Surf. Sci. 162 (1985) 348.
[21] K. H. Johnson, S. V. Pepper, J. Appl. Phys. 83 (1982) 6634.
[22] J. A. Kelber, C. Niu, K. Shepherd, D. R. Jennison, A. Bogicevic, Surf. Sci. 446 (1999) 76.
[23] J. W. Elam, C. E. Nelson, M. A. Cameron, M. A. Tolber, S. M. George, J. Phys. Chem. B 102 (1998) 7008.
[24] K. C. Hass, W. F. Schneider, A. Curioni, W. Andreoni, Science 282 (1998) 265.
[25] C. J. Powell, Surf. Interface Anal. 23 (1995) 121.
[26] D. Martini, K. Shepherd, R. Sutcliffe, J. A. Kelber, H. Edwards, R. S. Martin, Apllied Surf. Sci. 141 (1999) 89.
[27] J. Cazaux, P. Lehuede, J. Electron Spectrosc. Relat. Phenom. 59 (1992) 49.
[28] A. J. Pertsin, Y. M. Pashunin, Applied Surf. Sci. 44 (1990) 171.
[29] T. L. Barr, J. Vac. Sci. Technol. A 7 (1989) 1677.
[30] X. Yu, H. Hantsche, Surf. Interface Anal. 20 (1993) 555.
[31] A. P. Pijpers, K. Berreshelm, M. Wilmers, Fresenius J. Anal. Chem. 346 (1993) 104.
[32] P. Hohenberg, W. Kohn, Phys. Rev. 136 (1964) B864.
[33] W. Kohn, L. J. Sham, Phys. Rev. 140 (1965) A1133.
[34] J. P. Perdew, A. Zunger, Phys. Rev. B 23 (1981) 5048.
[35] D. M. Ceperley, B. J. Alder, Phys. Rev. Lett. 45 (1980) 566.
[36] G. Kresse, J. Hafner, Phys. Rev. B 47 (1993) 558.
[37] G. Kresse, J. Hafner, Phys. Rev. B 49 (1994) 14251.
[38] G. Kresse, J. Hafner, Phys. Rev. B 54 (1996) 11169.
[39] D. Vanderbilt, Phys. Rev. B 32 (1985) 8412.
[40] D. Vanderbilt, Phys. Rev. B 41 (1990) 7892.
[41] J. Ahn, J. W. Rabalais, Surf. Sci. 388 (1997) 121.
[42] J. M. McHale, A. Auroux, A. J. Perrotta, A. Navrotsky, Science 277 (1997) 788.
[43] J. F. Moulder, W. F. Stickle, P. E. Sobol, K. D. Bomben, J. Chastain, R. C. King, Handbook of X-ray photoelectron spectroscopy, Physical Electronics, Inc., Eden Prairie, Minnesota 1995.
[44] K. Wandelt, Surf. Sci. Rep. 2 (1982) 1.
[45] A. Bogicevic, D. R. Jennison, Surf. Sci. 437 (1999) L741.
[46] C. E. Nelson, J. W. Elam, M. A. Cameron, M. A. Tolbert, S. M. George, Surf. Sci. 416 (1998) 341.
[47] B. G. Frederick, G. Apai, T. N. Rhodin, Surf. Sci. 277 (1992) 337.
[48] P. Liu, T. Kendelewicz, J. G.E. Brown, E. J. Nelson, S. A. Chambers, Surf. Sci. 417 (1998) 53.
[49] C. T. Campbell, (unpublished results) .